Chemical Geology 287 (2011) 81–89

Contents lists available at ScienceDirect

Chemical Geology

journal homepage: www.elsevier.com/locate/chemgeo

Mercury distributions and mercury isotope signatures in sediments of Dongjiang, the Pearl River Delta, China

Jinling Liu [a,b], Xinbin Feng [a,*], Runsheng Yin [a,b], Wei Zhu [a,b], Zhonggen Li [a]

[a] State Key Laboratory of Environmental Geochemistry, Institute of Geochemistry, Chinese Academy of Sciences, Guiyang 550002, China
[b] Graduate University of Chinese Academy of Sciences, Beijing 100049, China

ARTICLE INFO

Article history:
Received 29 December 2010
Received in revised form 26 May 2011
Accepted 2 June 2011
Available online 12 June 2011

Edited by J.D. Blum

Keywords:
Mercury
Methylmercury
Isotope tracing
The Pearl River Delta

ABSTRACT

The Pearl River Delta (PRD) is one of the most industrialized and urbanized regions in China. In order to assess the pollution status of mercury (Hg) in PRD river system, the distribution of total mercury (HgT) and methylmercury (Me-Hg) in sediment from a large river named Dongjiang (DJ) was for the first time investigated. HgT concentrations in sediment increased from the upstream to downstream of Dongjiang area and at most sites of DJ were significantly higher than the background values, which suggested that the DJ was contaminated with Hg, especially in the downstream of DJ. Me-Hg concentrations in sediment of DJ ranged from 0.56 to10.62 ng/g, and were significantly correlated with HgT and organic matter. In order to determine the potential Hg contamination sources, typical sediments from different parts of DJ were chosen for Hg isotope analysis. The results showed that the mass-dependent fraction (MDF) in the sediments varied significantly (δ^{202}Hg: −2.35 to−0.60‰), and the mass-independent fraction (MIF) in the sediments also varied considerably (Δ^{199}Hg: −0.02 to −0.27‰). The samples with the highest HgT located in the industrial area had the highest δ^{202}Hg (−1.14‰ to −0.60‰) measured values and insignificant MIF (Δ^{199}Hg: −0.04 to −0.01‰). Meanwhile, the samples with the lowest HgT located in the background area had the lowest δ^{202}Hg (−2.16‰ to −1.55‰) and Δ^{199}Hg (−0.20 to −0.27‰) measured values. Unlike the above two cases are the samples located in the urban area, which have relative lower MDF (δ^{202}Hg: −2.35‰ to −1.96‰) and small but significant MIF (Δ^{199}Hg: −0.10‰ to −0.08‰) with relative higher HgT. We demonstrated that the dominant Hg sources in DJ sediments could be categorized as the regional background, urban and industrial sources. In our study, we demonstrated that Hg stable isotope method could serve as an effective tool for tracing mercury contamination sources in the environment.

1. Introduction

Mercury (Hg) is one of the most toxic heavy metals in the environment and represents a global contamination problem (Lindqvist et al., 1991; Conaway et al., 2003; Li et al., 2009). Due to rapid urbanization and industrialization, China has become one of the largest mercury emission countries in the world (Feng, 2005; Streets et al., 2005; Zhang and Wong, 2007). The Pearl River Delta (PRD) region, which is located in Guangdong province, consisting of Guangzhou, Shenzhen, Zhuhai, Foshan, Dongguan, Zhongshan, Huizhou, Jiangmen and Zhaoqing cities, is currently one of the most industrialized and urbanized regions in China (NDRC, 2008). In PRD, the rapid development of economy has led to seriously contamination of heavy metals (such as Pb, Zn, Cu, and Cr) in the environment (Ip et al., 2005, 2007). During the past two decades, a large amount of Hg was used in chlor-alkali industries, manufacture of electrical products, alloy materials, chemical reagents, medicines, clothing, toys, and other goods for the global market (China Environment Year-book Committee, 1990–1997; Zhou and Wong, 2000; Streets et al., 2005; Zhang and Wong, 2007). Hg was released into the surrounding environment by waste water discharge and flue gas emissions. These activities resulted in Hg contamination to the local environment and the adjacent ecosystems, including contamination to air, water, soil, sediment, and organisms (Zhou and Wong, 2000; Shi et al., 2010a, 2010b).

Previous studies showed that sediment was not only an efficient sink for atmospheric Hg deposition and waste water discharge, but also a source of methylmercury (Me-Hg) to the water column (Covelli et al., 1999; Mason et al., 1999; Hines et al., 2000; Tomiyasu et al., 2000; Macleod et al., 2005; Merritt and Amirbahman, 2007; Ullrich et al., 2007; Shi et al., 2010a, 2010b). The anoxic condition of sediment may enhance the bacterial methylation processes that convert inorganic Hg to its more toxic form, Me-Hg which is a neurotoxin for humans (Mason et al., 2006). Me-Hg produced in sediment can be transported to the water column and then be bioaccumulated by aquatic organisms (Pickhardt and Fisher, 2007; Chen et al., 2009) and biomagnified in food webs (Lawson and Mason, 1998). Fish consumption is thought to

* Corresponding author. Tel.: +86 851 5891356; fax: +86 851 5891609.
E-mail address: fengxinbin@vip.skleg.cn (X. Feng).

0009-2541/$ – see front matter © 2011 Elsevier B.V. All rights reserved.
doi:10.1016/j.chemgeo.2011.06.001

be the most important Me-Hg exposure pathway in developed countries (Clarkson and Magos, 2006).

With the development and application of multiple collector inductively coupled plasma mass spectrometry (MC-ICP-MS), accurate and precise measurements of isotope ratios of heavy elements have been made possible. Meanwhile, natural fractionation of Hg isotopes has been the subject of many studies and Hg isotope ratios have been measured in materials including hydrothermal ores (Smith et al., 2005, 2008), coal samples (Biswas et al., 2008), soils (Foucher et al., 2009), volcanic emission (Zambardi et al., 2009), sediments (Ghosh et al., 2008; Gehrke et al., 2009), and biological samples (Bergquist and Blum, 2007; Carignan et al., 2009). Hg isotopes are fractionated by natural processes such as volatilization (Zheng et al., 2007), reduction induced by chemical (Yang and Sturgeon, 2009), photochemical (Bergquist and Blum, 2007) and bacterial processes (Kritee et al., 2007, 2009). In addition to these natural processes, industrial processes could also generate Hg isotope fraction, resulting in specific isotope ratios in a region or an industry (Estrade et al., 2010). The fingerprinting characteristics of Hg isotope signatures have been demonstrated to be a good tool of tracing the sources and biogeochemical processes of Hg in the environment (Bergquist and Blum, 2007; Blum and Bergquist, 2007; Foucher et al., 2009; Stetson et al., 2009; Estrade et al., 2010; Feng et al., 2010; Sonke et al., 2010). Moreover, Perrot et al. (2010) have shown that Hg isotopes can be also used to track anthropogenic sources of Hg accumulating from the sediments to fish.

In PRD, as one of three largest tributaries of Pearl River, Dongjiang (DJ) is an important water resource to the local inhabitants. However, the status of Hg pollution, as well as the potential Hg contamination sources in sediments of DJ, is still poorly understood. The goals of this study are 1) to investigate the Hg contamination status in sediment of DJ; 2) to evaluate the potential of Hg methylation in sediment; 3) and to understand the sources of Hg pollution in DJ.

2. Methods

2.1. Study area and sampling

DJ has a length of 562 km and flows through the PRD. Fifty three sediment samples (Marked as A, B, C, D, E and Z) were collected from the upstream to downstream of Dongjiang area in July 2009 (Fig. 1). As shown in Fig. 1, the sediment samples in DJR were classified into three groups. The first group, the upper and middle stream of Dongjiang area, consists of segment Z (Z1–Z4, Z6–Z7, Z14, n = 7) and segment F (A9, E16, E18, E19, n = 4). The second group, the industrial zone of Dongguan city, consists of segment A (A1–A6, n = 6), segment B (B1–B5, n = 5), segment C (C1–C8, n = 8), and segment D (D1–D8, n = 8). The third group, the urban area of Dongguan city, includes segment E (E1–E15, n = 15).

At each sampling site, a composite sample was composed of 5 subsamples (i.e., quincunx) collected within an area of about 3–5 m^2. During the sampling campaign, each sample was collected in a sealed polyethylene bag to avoid cross contamination and stored frozen in a cooler. In the laboratory, samples were freeze dried, homogenized, and sieved to minus 100 mesh prior to chemical analysis.

2.2. Organic matter analysis

The organic matter concentrations in all samples were determined by measuring the gravimetric loss on ignition at 550 °C over 4 h (Boyle, 2004).

2.3. Total Hg and Me-Hg concentration analysis

The total mercury (HgT) concentrations in sediments were determined on the solid samples by Lumex RA 915$^+$ mercury analyzer equipped with a two-chamber pyrolysis block (Lumex Ltd., Russia), following a method reported by Luis et al. (2007). Briefly, the samples were heated to 800 °C in a first heating chamber, leading to the volatilization of the Hg and organic compounds of the sample. All products were transported from the first chamber to a second one by an air flow. The second chamber was continuously heated at about 800 °C. There, smoke and interference compounds were burnt, producing mostly carbon dioxide and water. Hg in the gas flow was determined by flameless atomic absorption spectrometry. A Zeeman corrector of the spectrometer eliminated the rest of the background absorption. The detection limit for HgT was 0.5 ng/g. All the samples were analyzed in triplicate. Accuracy was assessed using the certified reference materials GBW 07305 and GBW 07405 (IGGEC, Institute of Geophysical and Geochemical Exploration, China), with an average percent recovery of 89.5% (Table 1).

The concentrations of Me-Hg in sediments were determined by acidic extraction, ethylation, isothermal GC separation and CVAFS detection (Liang et al., 2004). Recoveries for matrix spikes are 80% to 116% for Me-Hg. The certified reference materials, including marine sediments of BCR-580 (IRMM, Institute of Reference Materials and Measurements) and IAEA-356 (IAEA, Marine Environment Laboratory, International Atomic Energy Agency), were used for quality control of sediment sample (Table 1).

2.4. Hg isotope analysis

Hg isotopic ratios were determined by MC-ICP-MS using a Nu-Plasma mass spectrometer equipped with twelve Faraday cups (Nu Instruments, Great Britain) at the State Key Laboratory of Environmental Geochemistry, Institute of Geochemistry, Chinese Academy of Sciences, China. The sample introduction system consisted of a continuous flow cold-vapor generation system (CV) (HGX-200, CETAC U.S.) coupled to an Apex-Q desolvation unit (Elemental Scientific Inc., U.S.) for Hg and Tl introduction, respectively. $SnCl_2$ was used as reducing agent and mixed online with Hg standards or sample digests to generate volatile elemental Hg. Hg vapors from the CV generation system were mixed with a dry Tl aerosol produced via the desolvation device. Instrumental mass bias correction was achieved using Tl as an internal standard and external standard-sample bracketing with a NIST SRM 3133 Hg solution. An exponential fractionation law was applied for internal mass bias correction assuming a reference value of 2.38714 for the ratio $^{205}Tl/^{203}Tl$. Data were acquired by monitoring ^{198}Hg, ^{199}Hg, ^{200}Hg, ^{201}Hg, ^{202}Hg, ^{203}Tl and ^{205}Tl isotopes for a period of 10 min (1 block, 100 cycles with 6 s integrations). A typical sequence consisted of measuring the NIST SRM 3133 Hg solution before and after each sample. To ensure optimum results of instrumental mass bias correction, the concentration of the bracketing solution was systematically adjusted to within 10% difference with the Hg concentration in the sample digest (typically 5 μg/L). Instrument blanks were analyzed after each sample and each bracketing standard and on-line subtracted. Typical blank values were 10 mV for ^{202}Hg and 30 mV for ^{205}Tl, insignificant relative to typical sample and standard signals of 1 V for ^{202}Hg and 3 V for ^{205}Tl. A more detailed description of the overall instrumental setup, as well as the parameters and analytical conditions used throughout this study can be found in Yin et al. (2010).

Hg isotopic variations are reported here in delta notation in units of permil (‰) and referenced to the NIST SRM 3133 Hg standard (analyzed before and after each sample) and using the following equation:

$$\delta^{xxx}Hg(‰) = \left\{\left(^{xxx}Hg/^{198}Hg_{sample}\right)/\left(^{xxx}Hg/^{198}Hg_{NISTSRM3133}\right)-1\right\}\times 1000 \quad (1)$$

where xxx is mass of each Hg isotope between 199 and 202 amu. Here only $\delta^{202}Hg$ values will be reported to indicate mass dependent fractionation (MDF) as they show the most significant differences

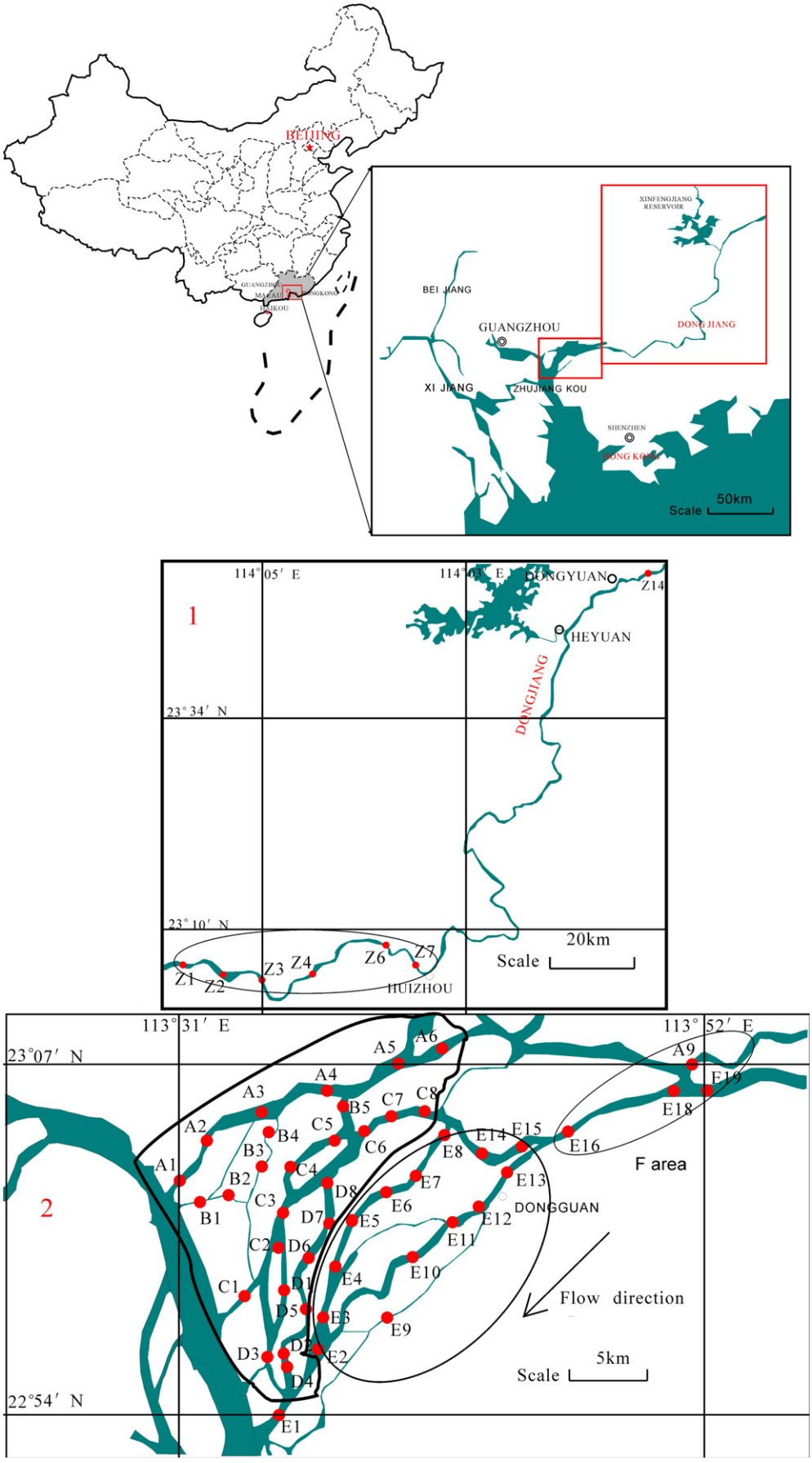

Fig. 1. Location of sampling sites in Dongjiang.

Table 1
Quality assurance data for analysis of total Hg and MeHg in certified reference materials.

Producer	Reference material	n	Hg speciation	Analytical results* (mg/kg)	Certified value* (mg/kg)
[a]IGGEC	GBW07405	9	Total Hg	0.28 ± 0.026	0.29 ± 0.04
[a]IGGEC	GBW07305	6	Total Hg	0.088 ± 0.008	0.1 ± 0.02
[b]IRMM	BCR-580	7	MeHg	0.063 ± 0.005	0.075 ± 0.004
[c]IAEA	IAEA-356	7	MeHg	0.0055 ± 0.00016	0.0054 ± 0.00089

*Values represent means ± standard errors.
[a] IGGEC: Institute of Geophysical and Geochemical Exploration, China.
[b] IRMM: Institute for Reference Materials and Measurements.
[c] IAEA: MEL International Atomic Energy Agency.

among samples. For the odd isotopes (^{199}Hg and ^{201}Hg), the measured isotope ratios occasionally deviated from MDF. In these instances, δ^{202}Hg is used to determine the predicted mass-dependent values of δ^{201}Hg and δ^{199}Hg using a kinetic mass-dependent fractionation law. Mass independent fractionation (MIF) is reported in "capital delta" notation (Δ^{xxx}Hg, deviation from mass dependency in units of permil, ‰) and is the difference between the measured δ^{xxx}Hg and the theoretically predicted δ^{xxx}Hg value using the following formulas (Blum and Bergquist, 2007):

$$\Delta^{201}\mathrm{Hg} \approx \delta^{201}\mathrm{Hg} - \left(\delta^{202}\mathrm{Hg} * 0.752\right) \quad (2)$$

$$\Delta^{199}\mathrm{Hg} \approx \delta^{199}\mathrm{Hg} - \left(\delta^{202}\mathrm{Hg} * 0.252\right). \quad (3)$$

Reproducibility of the isotopic data was assessed by measuring replicate sample digests (typically n = 2). We also analyzed the UM-Almadén as a secondary standard (once every 10 samples) in addition to the bracketing standard NIST 3133. Hg in UM-Almadén was measured the same way as other samples in each analytical session. As seen in Table 2, the overall average and uncertainty of δ values for all UM-Almadén measurements are well agreed with data reported by Blum and Bergquist (2007). Uncertainties reported in the figures and tables of this paper correspond to the larger value of either 1) the measurement uncertainty of replicate sediment digests, or 2) the uncertainty of repeated measurements of the same digest at different analysis sessions. When the calculated 2SD was smaller than the replicate analyses of the reference material of UM-Almaden, the uncertainty associated to UM-Almaden was used instead.

All sediment samples were digested with a fresh mixture of HNO_3–HCl (1:3, V/V) in a water bath (95 °C) for HgT analysis, and were diluted to yield a final Hg concentration of at least 5 μg/L before MC-ICP-MS analysis. This dilution was necessary to keep the acid concentration below 20% (v/v), above which matrix interferences affect Hg isotopic measurements. All acids used in this work were of guaranteed grade (HNO_3 and HCl). Mill-Q water (18.2MΩ·cm) and high purity argon were used. A 0.16 M (3% w/v) solution of stannous chloride was prepared in 1.20 M HCl. The reductant solution was purged prior to use with Hg-free nitrogen for a few hours in order to release mercury traces. The mercury (5 μg/L, NIST SRM 3133) and thallium (20 μg/L, NIST SRM 997) working standard solutions in 0.12 M HCl were prepared daily (Blum and Bergquist, 2007). A secondary standard solution (UM-Almadén, 1.0 μg/g Hg in 4% nitric acid) was obtained from University of Michigan. All Teflon materials and glassware were cleaned using HNO_3 (10%, v/v) and HCl (10%, v/v) for 48 h and triply rinsed with Milli-Q water (Yin et al., 2010).

3. Results and discussion

3.1. HgT in sediments

The distribution of HgT concentrations in sediments (n = 53) from the upstream to downstream of Dongjiang area is shown in Fig. 2 and Table S1. HgT concentrations in sediment samples were highly variable, ranging between 15 and 2000 ng/g. The statistical summary of HgT concentrations in sediment in all segments is listed in Table 3 and a general increase pattern of HgT concentrations in sediment from the upstream to downstream of Dongjiang area was noted.

As shown in Fig. 2, the lowest HgT concentrations in sediment were observed in the upper and middle reaches of Dongjiang area. The mean HgT concentration in sediment in this area (segments F and Z) was 76 ± 47 ng/g, which was similar to the background HgT concentration in the PRD (58 ng/g, Shi et al., 2007). Despite the relative high HgT concentration in Huizhou city (189 ng/g at Z7), all the other sediment samples in segments F and Z had low HgT concentrations, which were lower than the Grade 1 level for soil quality in China (150 ng/g, CNEPA, 1995), suggesting that sediments

Table 2
Mercury isotope composition for samples of Dongjiang River sediments and UM-Almadén (N = 15) and BCR 580 (N = 2).

Sample number	δ^{199}Hg	2SD	δ^{200} Hg	2SD	δ^{201} Hg	2SD	δ^{202} Hg	2SD	Δ^{199} Hg	2SD	Δ^{200} Hg	2SD	Δ^{201} Hg	2SD	HgT	Me-Hg
	‰	‰	‰	‰	‰	‰	‰	‰	‰	‰	‰	‰	‰	‰	(μg/g)	(ng/g)
A1	−0.18	0.00	−0.43	0.02	−0.63	0.05	−0.80	0.10	−0.02	0.03	−0.02	0.03	−0.03	0.03	0.40	0.92
A3	−0.31	0.05	−0.59	0.11	−0.88	0.18	−1.14	0.21	−0.02	0.03	−0.02	0.00	−0.03	0.03	0.20	4.03
A4	−0.27	0.02	−0.52	0.03	−0.75	0.01	−1.00	0.10	−0.02	0.03	−0.01	0.01	0.00	0.03	0.45	3.05
A5	−0.25	0.04	−0.46	0.09	−0.71	0.07	−0.91	0.12	−0.02	0.03	0.00	0.03	−0.03	0.03	0.55	1.86
A7	−0.18	0.04	−0.37	0.10	−0.54	0.13	−0.67	0.16	−0.01	0.03	−0.03	0.02	−0.03	0.03	1.32	2.75
B2	−0.38	0.05	−0.54	0.07	−0.92	0.09	−1.12	0.16	−0.04	0.03	−0.03	0.01	−0.03	0.03	0.21	2.75
B3	−0.30	0.03	−0.58	0.08	−0.87	0.08	−1.14	0.10	−0.02	0.03	−0.01	0.03	−0.01	0.03	0.34	3.05
C1	−0.21	0.03	−0.38	0.07	−0.57	0.13	−0.71	0.16	−0.03	0.03	−0.02	0.01	−0.03	0.03	0.41	2.03
C7	−0.17	0.03	−0.32	0.04	−0.50	0.08	−0.60	0.10	−0.02	0.03	−0.02	0.01	−0.05	0.03	1.97	10.62
C8	−0.20	0.04	−0.35	0.10	−0.56	0.15	−0.72	0.19	−0.02	0.03	0.01	0.00	−0.02	0.03	2.00	4.46
D6	−0.37	0.00	−0.50	0.02	−0.84	0.07	−1.00	0.10	−0.03	0.03	−0.02	0.02	0.03	0.03	0.40	1.43
D8	−0.27	0.08	−0.44	0.14	−0.69	0.15	−0.90	0.19	−0.04	0.03	0.01	0.05	−0.02	0.03	0.97	2.51
Z1	−0.48	0.01	−0.81	0.03	−1.25	0.08	−1.55	0.10	−0.24	0.03	0.00	0.03	−0.18	0.03	0.10	0.89
Z4	−0.60	0.03	−0.96	0.01	−1.59	0.09	−1.99	0.10	−0.20	0.03	0.02	0.01	−0.16	0.03	0.08	2.16
Z7	−0.56	0.02	−1.06	0.05	−1.58	0.01	−2.06	0.10	−0.21	0.05	0.04	0.02	−0.19	0.03	0.19	2.03
Z14	−0.68	0.04	−1.12	0.04	−1.73	0.04	−2.16	0.10	−0.27	0.03	−0.03	0.01	−0.21	0.04	0.15	1.98
E2	−0.62	0.14	−1.21	0.26	−1.74	0.37	−2.35	0.49	−0.08	0.03	−0.03	0.02	−0.07	0.03	0.52	1.22
E9	−0.57	0.02	−1.02	0.06	−1.54	0.13	−1.96	0.12	−0.10	0.03	0.01	0.06	−0.10	0.03	0.59	3.02
E11	−0.58	0.01	−0.93	0.03	−1.52	0.12	−1.88	0.17	−0.09	0.03	−0.03	0.01	−0.09	0.03	0.41	1.92
E12	−0.66	0.05	−1.19	0.14	−1.81	0.14	−2.31	0.23	−0.08	0.03	−0.04	0.00	−0.07	0.04	0.49	2.06
UM-Almadén	−0.15	0.06	−0.25	0.04	−0.39	0.07	−0.53	0.08	−0.01	0.02	0.02	0	0.01	0.03	–	–
BCR 580	−0.14	0.01	−0.24	0.02	−0.38	0.03	−0.46	0.04	−0.02	0.01	−0.01	0.02	−0.03	0.02	–	–

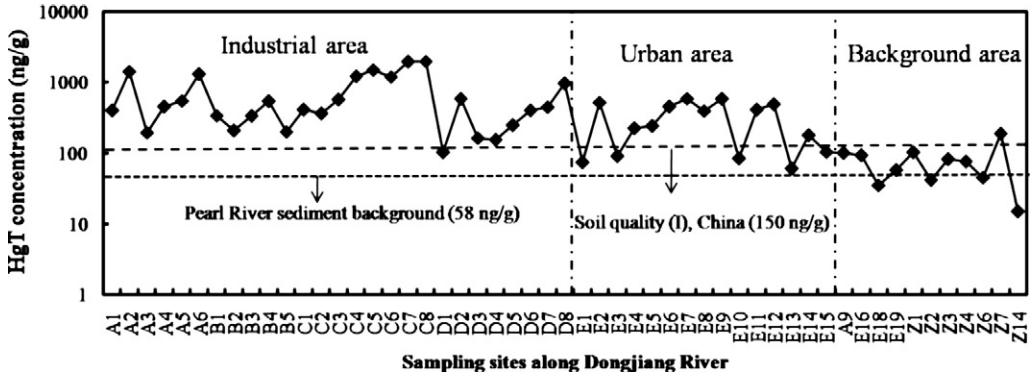

Fig. 2. Distribution of HgT in sediments of Dongjiang.

at the upstream and middle stream of Dongjiang area were less contaminated by anthropogenic activities.

As shown in Fig. 1, the DJ was separated into several parallel rivers that flowed through Dongguan area at downstream of Dongjiang area. Elevated HgT concentrations in sediment were observed in the downstream of Dongguan area (Table 3). Being one of the fastest developing cities in China, Dongguan is famous for its industries for electronic appliances, chemical plants, paper mills, pharmaceuticals, and waste incineration. Generally, those industries were situated to be far away from the urban areas due to environmental concerns. During the past two decades, the waste water discharged from these industries were not properly treated and had led to elevated HgT concentrations in sediment of this region (mean HgT, 677 ± 561 ng/g), especially in segments A, B, C and D (Table 3). The highest value of HgT concentration in sediment was found at segment C (Fig. 2), where the most chemical plants, paper mills, and plastic plants are located. Meanwhile, considering that C8 and C7 were located closely to the point sources of mercury in the segment C, a decrease pattern of HgT in sediments was observed from site C8 to C1 (Fig. 2). A similar pattern was also observed in other segments (such as Segments A, B, and D).

Different from segments A, B, C, and D, the segment E was located in the urban area of Dongguan city (Fig. 1). In this region, although there are no industrial point sources of Hg contamination, the densely populated urban area may still contribute a large amount of Hg to the environment through multiple pathways such as coal combustion, automobile emission, refuse dump and domestic sewage. This was consistent with the relative high HgT concentrations (mean 301 ± 200 ng/g) in sediment in segment E that was less contaminated compared to the industrial areas.

3.2. Me-Hg in sediments

Me-Hg concentrations in surface sediments of DJ ranged from 0.56 to 10.62 ng/g (Tables 3 and S1). The Me-Hg concentrations in sediment (with an average of 2.96 ± 2.05 ng/g) in the industrial area (including segments A, B, C, and D) were at the same level as that of another heavy industry area, the Haihe River, China (0.8–7.7 ng/g) (Shi et al., 2005). However, the Me-Hg levels observed in this study were much higher than those of other rivers including some highly heavily mercury contaminated areas. For example, Me-Hg concentrations in sediments from downstream of Palawan Hg mine in Philippines only ranged from 0.28 to 3.9 ng/g (Gray et al., 2003). Me-Hg concentrations in DJ were also higher than those found in the sediments of San Francisco Bay estuary (0.108–1.08 ng/g) and Sacramento River (0.27–2.84 ng/g) in US (Domagalski, 2001; Conaway et al., 2003).

Generally, the ratio between Me-Hg/HgT in sediments is less than 1% (Hines et al., 2000; Zelewski et al., 2001; Niessen et al., 2003; Ullrich et al., 2007), except for some lakes and wetlands where the percentage of MeHg can reach up to 10% (Ullrich et al., 2001; Fischer and Gustin, 2002). In DJ sediments, the mean value of Me-Hg/HgT ratio was 1.25% (0.11%–13.17%). A significant positive correlation ($r^2 = 0.29$, $p < 0.01$, n = 53) between Log (Me-Hg) and Log (HgT) in sediments of DJR was observed in Fig. 3a. It was also shown in Fig. 3b that the correlation ($r^2 = 0.12$, $p < 0.05$, n = 51) between Log (Me-Hg) and Log (OM) (Organic Matter) was significantly positive. These suggested that 29% of Me-Hg variation was explained by HgT and 12% by organic matter (OM). As HgT concentration and OM content appear to small but significant influence on Me-Hg production, the overriding control in the DJ system is likely microbiological activity.

Table 3
HgT and MeHg concentrations, δ^{202}Hg values in sediments collected from Dongjiang River.

Part	Area	Segment	HgT concentration (ng/g)				Me-Hg concentration (ng/g)				δ^{202}Hg	Δ^{199}Hg
			min	max	mean	median	min	max	mean	median	Interval	Interval
Downstream of Dongjiang River	Industrial zone of Dongguan city	A (n = 6)	195	1435	726 ± 519	502	0.92	4.88	2.92 ± 1.43	2.9	−1.14‰ to −0.60‰ (n = 12)	−0.04‰ to −0.01‰ (n = 12)
		B (n = 5)	200	543	326 ± 139	336	1.81	4.9	3.05 ± 1.13	2.76		
		C (n = 8)	367	2000	1154 ± 656	1205	1.65	10.62	4.39 ± 2.90	3.75		
		D (n = 8)	102	972	384 ± 290	326	0.97	2.51	1.52 ± 0.58	1.26		
		Total (n = 27)	102	2000	677 ± 561	449	0.92	10.62	2.96 ± 2.05	2.72		
	Urban area of Dongguan city	E (n = 15)	60	593	301 ± 200	242	0.92	3.02	1.63 ± 0.57	1.61	−2.35‰ to −1.96‰ (n = 4)	−0.10‰ to −0.08‰ (n = 4)
Upper and middle streams of Dongjiang River		F (n = 4)	35	100	71 ± 31	75	0.56	2.31	1.52 ± 0.86	1.6	−2.16‰ to −1.55‰ (n = 4)	−0.27‰ to −0.20‰ (n = 4)
		Z (n = 7)	15	189	79 ± 57	76	0.89	2.16	1.56 ± 0.55	1.79		
		Total (n = 11)	15	189	76 ± 47	76	0.56	2.31	1.54 ± 0.63	1.79		
Dongjiang overall (n = 53)			15	2000	446 ± 481	336	0.56	10.62	2.29 ± 1.66	1.92		

3.3. Tracing Hg sources by using Hg isotope ratios

Mercury isotope compositions in surface sediments of the DJ are presented in Table 2. The potential explain for the measured Hg isotope deviations would be geochemical processes resulting in a fractionation of Hg isotopes. For example, microbial reduction (Kritee et al., 2007, 2009), photoreduction (Bergquist and Blum, 2007), and evasion processes (Zheng et al., 2007) preferentially act on the light Hg isotopes, which subsequently leave the system. However, a recent study suggested that partitioning of Hg between solid and dissolved phases does not generate measurable Hg isotope fractionation in natural environments (Foucher et al., 2009). Thus, the distinct Hg isotope signatures observed from different locations of DJ may imply different dominating Hg contaminated sources at different locations of DJ. According to mercury isotope signatures, HgT concentrations, as well as the industrial distributions in the study area, the potential Hg contamination sources in different regions of DJ can be categorized.

In the upstream and middle stream of the Dongjiang area (segments F and Z), δ^{202}Hg values of sediments were characterized by the relative lower values (varying from −2.16‰ to −1.55‰). In addition to mass dependent fractionation (MDF), mass independent isotope fractionation (MIF) was also observed for the sediment samples from the upstream and middle stream of Dongjiang area as shown in Figs. 5 and 6 (Δ^{199}Hg = −0.20 to −0.27‰). The negative MIF values for pristine sediments are consistent with recent literatures, as Hg MIF appears to be a recurrent feature for continental non-contaminated sediments across the globe (Laffont et al., 2009; Sonke et al., 2010). MIF is generally understood to be caused by the nuclear field shift (Schauble, 2007) and/or the magnetic isotope effects (Buchachenko et al., 2007). Previous studies demonstrated that MIF is caused by photochemical reduction of reactive Hg^{+2} species and monomethylmercury (Me-Hg) to Hg^0. When Δ^{199}Hg vs Δ^{201}Hg is plotted for each of these photochemical reduction processes, a slope of 1.36 is observed for Me-Hg and 1.00 for Hg^{+2} photo-reduction (Bergquist and Blum, 2007). It is demonstrated that soil erosion and atmospheric deposition of Hg are important Hg sources to the sediments in pristine areas (Sunderland and Mason, 2007). The Δ^{199}Hg vs Δ^{201}Hg plot of sediment samples from DJ has a slope of 0.823 as shown in Fig. 6 indicating that the cause of MIF could be photochemical reduction of Hg^{+2}, induced by magnetic isotope effects (Buchachenko et al., 2007). This would suggest that part of Hg in sediments of this region could have undergone photo-reduction process prior to being deposited to sediment.

In segments A, B, C, and D, air deposition and soil erosion may also contribute Hg to those segments; however, industries constitute the primary Hg contamination sources in sediments of this region as discussed in Section 3.1. The δ^{202}Hg values of sediment in segments A, B, C, and D ranged from −1.14‰ to −0.60‰, which is significantly different from the values in the pristine upstream and middlestream

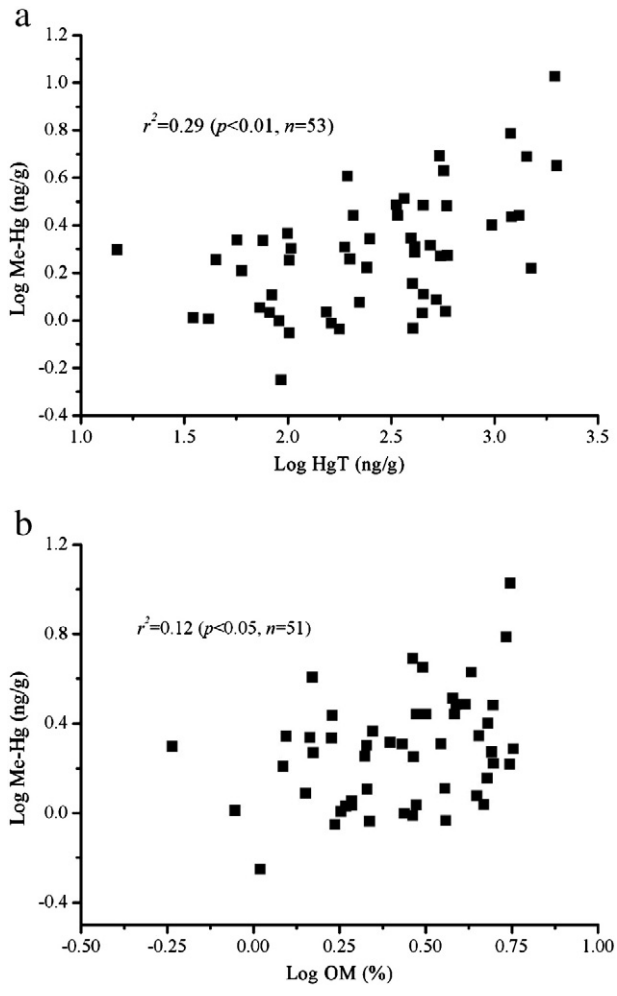

Fig. 3. Two-way scatter plots (a, b) for sediments from Dongjiang: a. Log (MeHg) (ng/g) vs. Log (HgT) (ng/g); b. Log (MeHg) (ng/g) vs. Log (Organic Matter) (%). Sample size (n) represents all data.

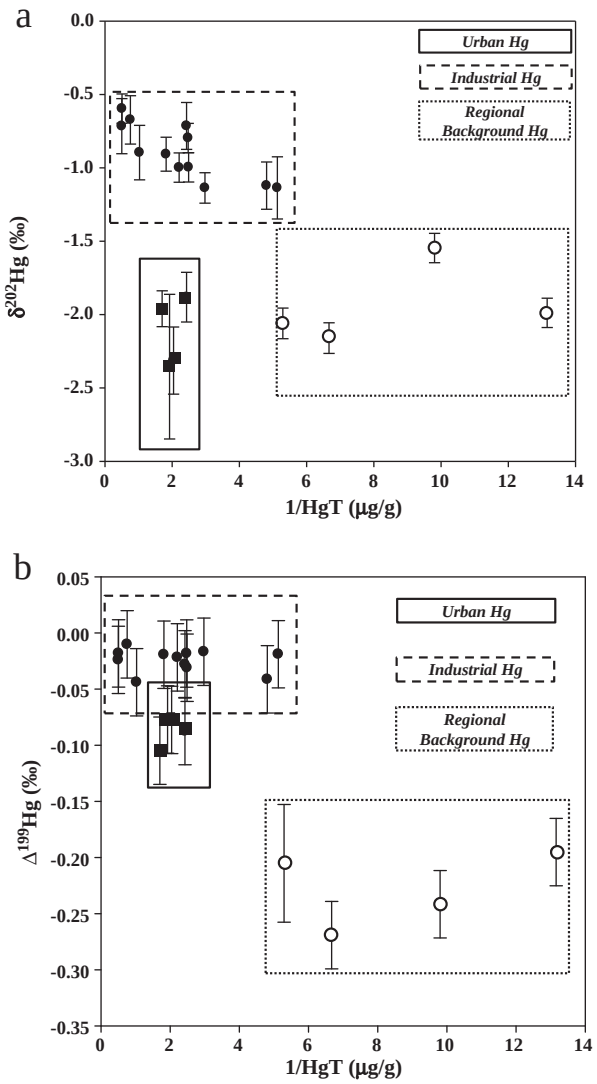

Fig. 4. a. Correlation between δ^{202}Hg and 1/HgT in sediments of Dongjiang. b. Correlation between Δ^{199} Hg and 1/HgT in sediments of Dongjiang.

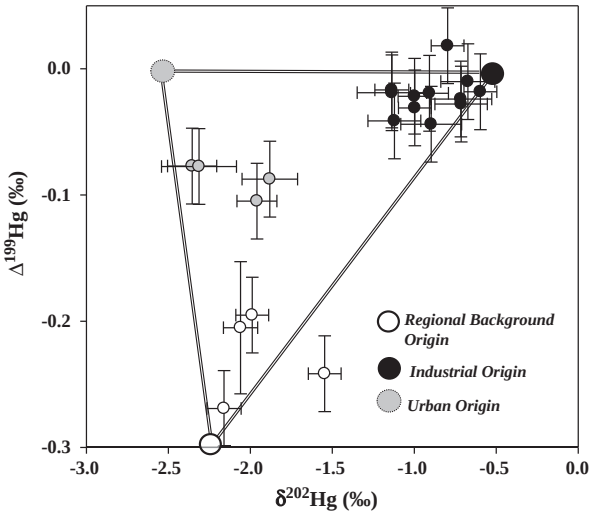

Fig. 5. Correlation between δ^{202}Hg and Δ^{199} Hg in sediments of Dongjiang.

of Dongjiang urban area. No MIF was observed in the industrial areas of Dongjiang urban area (Δ^{199}Hg = −0.04 to −0.01‰). We assume that Hg used in the industries of DJ was mainly from mercury mines. The relative heavier δ^{202}Hg values, as well as the absence of MIF in the segments A, B, C, and D compared to those of the upstream and middle stream of Dongjiang urban area, were well consistent with previous studies, from which the analyses of Hg ores, other metal deposits, did not show significant MIF (Hintelmann and Lu, 2003; Smith et al., 2005, 2008; Stetson et al., 2009). This further supported that industrial Hg is the dominate source of Hg pollution to the sediments of this area.

As discussed in Section 3.1, the segment E flows through the Dongguan urban area were elevated by HgT (with a mean of 301 ± 200 ng/g) compared to that of Segments F and Z (with a mean of 76 ± 47 ng/g). By utilizing both MDF and MIF, specific mercury isotope signatures of sediments from segment E were observed and shown in Fig. 5. Different with the industrial region, the cause of the relative negative δ^{202}Hg values of the sediment in this area (with δ^{202}Hg ranging from −2.35‰ to −1.96‰) needs to be better augmented. However, the lower δ^{202}Hg values may have some implications on Hg source "fingerprints" of segment E. It has been reported by several studies that the dominant Hg

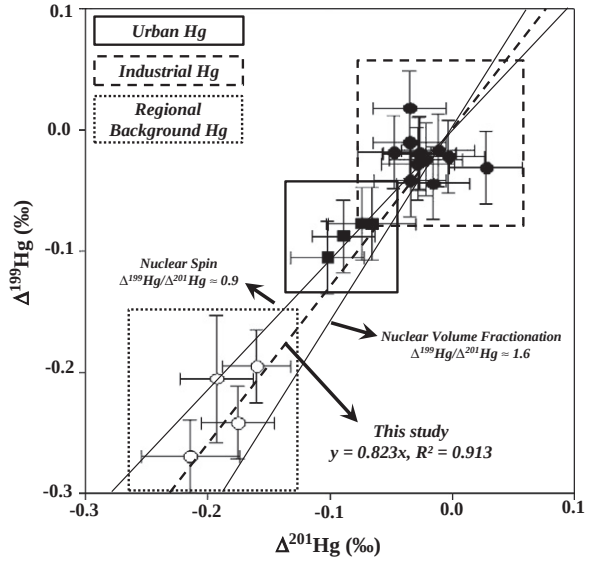

Fig. 6. Correlation between Δ^{199} Hg and Δ^{201} Hg in sediments of Dongjiang.

sources of this area are thought to be coal combustion emission, automobile emission and refuse dump conducted by the densely urban population (Zhou and Wong, 2000; Shi et al., 2010a, 2010b). They are probably corresponding with the lower δ^{202}Hg signature of segment E. Moreover, the MIF in segment E, with Δ^{199}Hg values ranging from −0.10‰ to −0.08‰, also showed a distinct signature with that of the upstream and middle stream (Δ^{199}Hg = −0.20 to −0.27‰) and industrial areas (Δ^{199}Hg = 0) of DJ as shown in Fig. 5.

Overall, the MDF in the sediments varied significantly (δ^{202}Hg = −2.35 to −0.60‰), and the MIF in the sediments also varied considerably (Δ^{199}Hg = −0.02 to −0.27‰). The sample with the highest HgT located in industrial area has also the highest δ^{202}Hg measured values (Fig. 4a) and insignificant MIF (Fig. 4b). Meanwhile, the sample with the lowest HgT located in the background area has also the lowest δ^{202}Hg and Δ^{199}Hg measured values (Fig. 4). Unlike the above two cases are the samples located in urban area, which have relative lower MDF and small but significant MIF with relative higher HgT (Fig. 4). As shown in Figs. 4 and 5, Hg in the sediments originates from a direct mixing between an Hg contamination source indicating industrial areas (1/HgT>0, −1.5‰<δ^{202}Hg<−0.5‰, Δ^{199}Hg of ~0‰), urban areas (1<1/HgT<3, −3.0‰<δ^{202}Hg<−1.5‰, −0.15‰<Δ^{199}Hg<−0.05‰) and the natural background soils (5<1/HgT<13, −2.5‰<δ^{202}Hg<−1.5‰, Δ^{199}Hg<−0.25‰). The explanation for the measured variations in Hg MDF/MIF could be the fact that the Hg in DJ sediments is a mixture of natural origin, urban origin, and industrial origin.

3.4. Triple mixing-model

As shown in Fig. 5, the combination of MDF/MIF signatures of the sediments indicated a triple mixing of natural, urban, and industrial Hg sources. Thus, the isotope compositions of the three end-members model determined as follow (Eqs. (4)–(6)) might be conducted to calculate the relative contribution of the three sources.

$$X\Delta^{199}Hg_{ind} + Y\Delta^{199}Hg_{urb} + Z\Delta^{199}Hg_{bac} = \Delta^{199}Hg_{sample} \quad (4)$$

$$X\delta^{202}Hg_{ind} + Y\delta^{202}Hg_{urb} + Z\delta^{202}Hg_{bac} = \delta^{202}Hg_{sample} \quad (5)$$

$$X + Y + Z = 1 \quad (6)$$

where X, Y, Z represent relative contribution of the sources industrial origin, urban origin, and regional background origin, respectively. Subscripts *ind, urb,* and *bac* refer to Hg with industrial origin, urban origin, and regional background origin. The coefficients in the equations set are defined by the isotope composition of the three end-members shown as x ($\Delta^{199}Hg_{ind}$, $\delta^{202}Hg_{ind}$), y ($\Delta^{199}Hg_{ant}$, $\delta^{202}Hg_{ant}$), and z ($\Delta^{199}Hg_{bac}$, $\delta^{202}Hg_{bac}$).

In previous study, simple MDF binary mixing models have been used successfully to estimate Hg pollution sources in many ecosystems (Foucher et al., 2009; Feng et al., 2010). These models are based on the precise characterization of two distinctive sources of Hg and these studies satisfactorily provided that each defined end-member has a significantly different isotopic composition. Appling this principle to our case study, we pointed out a z ($\Delta^{199}Hg_{bac}$: −0.27‰, $\delta^{202}Hg_{bac}$: −2.16‰) (Z14) to represent Hg with a regional background origin, because of the fact that Z14 is located at the head of the DJ with the lowest HgT. As the site C7 is located closely to the industry outlet with the highest HgT, x ($\Delta^{199}Hg_{ind}$: 0, $\delta^{202}Hg_{ind}$: −0.60‰) is chose to represent Hg with industrial origin. However, the Hg with urban origin could not be obtained directly from the sampling sites. As shown in Fig. 4a, the MDF signature of urban Hg is similar to the regional background, but different from the industrial Hg. However, the HgT concentrations in urban areas are much higher than the regional background values. It is implicated that Hg resources of urban area are partly similar to the regional background area. Thus in the urban area, a mixture of the urban origin (as discussed in Sections 3.1

and 3.3) and the regional background origin contributes Hg in sediment. Hg isotope of urban origin could be calculated by using the traditional isotopic mass balance mixing equations:

$$\delta^{202}Hg_{sample} = X_{ant}\delta^{202}Hg_{urb} + X_{reg}\delta^{202}Hg_{reg} \quad (7)$$

$$1 = X_{urb} + X_{reg} \quad (8)$$

$$X_{urb} = 1 - HgT_{reg} / HgT_{sample} \quad (9)$$

$$\Delta^{199}Hg_{sample} = X_{urb}\Delta^{199}Hg_{urb} + X_{reg}\Delta^{199}Hg_{reg} \quad (10)$$

where ($\delta^{202}Hg_{sample}$, $\Delta^{199}Hg_{sample}$), ($\delta^{202}Hg_{urb}$, $\Delta^{199}Hg_{urb}$), and ($\delta^{202}Hg_{reg}$, $\Delta^{199}Hg_{reg}$) are the isotopic deviation values of the sample in urban area, and of the urban and regional background end-members, respectively; X_{urb} and X_{reg} are the respective urban and regional background Hg fractions in the sample from the urban area. HgT_{sample} and HgT_{reg} correspond to the concentrations of total Hg in the samples from the urban area and the regional background area, respectively. Considering in the urban area, the highest $\delta^{202}Hg$ and HgT values observed at site E2, $\delta^{202}Hg_{sample}$ are defined as −2.35‰, $\Delta^{199}Hg_{sample}$ is −0.08‰, and HgT_{sample} is 0.52 μg/g. Based on the same principle, the regional background end-member is represented by Z14 ($\delta^{202}Hg_{reg}$: −2.16‰, $\Delta^{199}Hg_{reg}$: −0.27‰, HgT_{reg}:0.15 μg/g). According to Eqs. (7)–(10), the Y end-member (the urban origin of Hg) established in this study is calculated and represented by y ($\Delta^{199}Hg_{ant}$: 0, $\delta^{202}Hg_{ant}$: −2.43‰). This calculated value of $\Delta^{199}Hg_{ant}$ is identical with the previous studies. In previous studies, available data from various samples indicate that direct emissions from major urban sources, such as waste incineration (Estrade et al., 2009), are not characterized by a significant MIF. Indeed, analysis of Hg ores, other metal deposits, refined Hg as well as condensed materials from urban waste incineration do not reveal any MIF (Smith et al., 2005, 2008; Sherman et al., 2009). Meanwhile, Biswas et al. (2008) demonstrated that Chinese coals have a negligible MIF that is close to 0. Consequently, it is reasonable to adopt that urban Hg sources have no significant MIF anomalies.

Based on above, the three end-members in the triple mixing MDF/MIF model were developed.

According to Eqs. (4)–(6), we could calculate the relative contribution of the three sources in the sediments of the studied area. As shown in Fig. 7 and Table S2, the dominant source in the industrial area is from industrial origin (69% to 99%), whereas the most of contribution is regional background origin in the background area (72% to 100%). It appears that a mixture of urban and regional background origins is dominant in urban areas. Our data clearly showed that Hg originated from different sources had distinct Hg isotope ratios and therefore Hg isotope compositions can be used to quantify the sources of Hg contamination to the sediment.

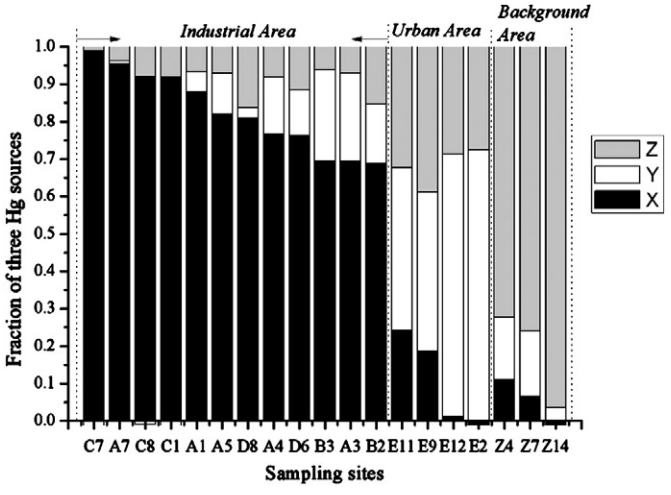

Fig. 7. Fractions of Hg sources in sediments of Dongjiang.

4. Conclusion

The HgT concentrations in the surface sediments of DJ were highly variable, ranging between 15 and 2000 ng/g. From the upstream to the downstream of Dongjiang urban area, the concentrations of HgT in sediment showed an increase trend. We also observed that sediment of river flowing through urban area at the downstream of DJ was less contaminated with Hg compared to the segments that flowing through the industrial areas. Industries at the downstream areas are the sources of Hg contamination to the river.

Me-Hg concentrations in surface sediments of DJ ranged from 0.56 to 10.62 ng/g and the mean value of MeHg/HgT ratio is 1.25%. Although both HgT and organic matter showed significantly positive correlation with Me-Hg in this study, only 29% of Me-Hg variation was explained by HgT and 12% by organic matter.

Hg isotope ratios were used to trace Hg contamination sources in sediments of DJR. Sediment at the downstream of DJR showed distinct Hg isotope ratios with the sediment at the upstream. This work further demonstrated that Hg isotope ratios can be used as a tool to trace the sources of Hg in the environment.

Supplementary materials related to this article can be found online at doi:10.1016/j.chemgeo.2011.06.001.

Acknowledgment

This study was financially supported by Chinese Academy of Sciences (KZCX2-YW-Q02-01) and National Natural Science Foundation of China (40825011, 21077103). We would like to thank Dr. Zhang Gan, Zeng Lingping, and Wang Jizhong of Guangzhou Institute of Geochemistry, Chinese Academy of Sciences; Dr. Zhang Xian and Luo Taiyi of Institute of Urban Environment, Chinese Academy of Sciences for their aid in the field sampling.

References

Bergquist, B.A., Blum, J.D., 2007. Mass-dependent and -independent fractionation of Hg isotopes by photoreduction in aquatic systems. Science 318, 417–420.
Biswas, A., Blum, J.D., Bergquist, B.A., Keeler, G.J., Xie, Z.Q., 2008. Natural mercury isotope variation in coal deposits and organic soils. Environ. Sci. Technol. 42, 8303–8309.
Blum, J.D., Bergquist, B.A., 2007. Reporting of variations in the natural isotopic composition of mercury. Anal. Bioanal. Chem. 388, 353–359.
Boyle, J., 2004. A comparison of two methods for estimating the organic matter content of sediments. J. Paleolimnol. 31, 125–127.
Buchachenko, A.L., Ivanov, V.L., Roznyatovskii, V.A., 2007. On the magnetic field and isotope effects in enzymatic phosphorylation. Dokl. Phys. Chem. 413, 39.
Carignan, J., Estrade, N., Sonke, J.E., Donard, O.F.X., 2009. Odd isotope deficits in atmospheric Hg measured in lichens. Environ. Sci. Technol. 243, 5660–5664.
Chen, C.Y., Dionne, M., Mayes, B.M., Ward, D.M., Sturup, S., Jackson, B.P., 2009. Mercury bioavailability and bioaccumulation in estuarine food webs in the Gulf of Maine. Environ. Sci. Technol. 43(6), 1804–1810.
China Environment Year-book Committee, 1990–1997. China environment yearbook. Chinese Environment Yearbook Committee Press, Beijing.
Clarkson, T.W., Magos, L., 2006. The toxicology of mercury and its chemical compounds. Crit. Rev. Toxicol. 36, 609–662.
CNEPA, China National Environmental Protection Agency, 1995. Environmental quality standard for soils. GB15618-1995. (In Chinese).
Conaway, C.H., Squire, S., Mason, R.P., Flegal, A.R., 2003. Mercury speciation in the San Francisco Bay estuary. Mar. Chem. 80, 199–225.
Covelli, S., Faganeli, J., Horvat, M., Brambati, A., 1999. Porewater distribution and benthic flux measurements of mercury and methylmercury in the Gulf of Trieste (northern Adriatic Sea). Estuar. Coast. Shelf Sci. 48, 415–428.
Domagalski, J., 2001. Mercury and methylmercury in water and sediment of the Sacramento River Basin, California. Appl. Geochem. 16, 1677–1691.
Estrade, N., Carignan, J., Sonke, J.E., Donard, O.F.X., 2009. Mercury isotope fractionation during liquid-vapor evaporation experiments. Geochim. Cosmochim. Acta 73, 2693–2711.

Estrade, N., Carignan, J., Donard, O.F., 2010. Isotope tracing of atmospheric mercury sources in an urban area of northeastern France. Environ. Sci. Technol. 44, 6062–6067.
Feng, X.B., 2005. Mercury pollution in China — an overview. In: Pirrone, N., Mahaffey, K. (Eds.), Dynamics of mercury pollution on regional and global scale: atmospheric process, human exposure around the world. Springer Publishers, Norwell, MA, pp. 657–678.
Feng, X.B., Foucher, D., Hintelmann, H., Yan, H.Y., He, T.R., Qiu, G.L., 2010. Tracing mercury contamination sources in sediments using mercury isotope compositions. Environ. Sci. Technol. 44, 3363–3368.
Fischer, P., Gustin, M.S., 2002. Influence of natural sources on mercury in water, sediment and aquatic biota in seven tributary streams of the East Fork of the Upper Carson River, California. Water Air Soil Pollut. 133, 283–295.
Foucher, D., Ogring, N., Hintelmann, H., 2009. Tracing mercury contamination from the Idrija mining region (Slovenia) to the gulf of Trieste using Hg isotope ratio measurements. Environ. Sci. Technol. 43, 33–39.
Gehrke, G.E., Blum, J.D., Meyers, P.A., 2009. The geochemical behavior and isotopic composition of Hg in a mid-Pleistocene western Mediterranean sapropel. Geochim. Cosmochim. Acta. 73, 1651–1665.
Ghosh, S., Xu, Y.F., Humayun, M., Odom, L., 2008. Mass-independent fractionation of mercury isotopes in the environment. Geochem. Geophys. Geosyst. 9 doi:10.1029/2007GC001827.
Gray, J.E., Greaves, I.A., Bustons, D.M., Krabbenhoft, D.P., 2003. Hg and methylmercury contents in mine-waste calcine, water, and sediment collected from the Palawan Quicksilver Mine, Philippines. Environ. Geol. 43, 298–307.
Hines, M.E., Horvat, M., Faganeli, J., Bonzongo, J.C.J., Barkay, T., Major, E.B., Scott, K.J., Bailey, E.A., Warwick, J.J., Lyons, W.B., 2000. Mercury biogeochemistry in the Idrija River, Slovenia, from above the mine into the Gulf of Trieste. Envrion. Res. 83, 129–139.
Hintelmann, H., Lu, S.Y., 2003. High precision isotope ratio measurements of mercury isotopes in cinnabar ores using multi-collector inductively coupled plasma mass spectrometry. Analyst 128, 635–639.
Ip, C.C.M., Li, X.D., Zhang, G., Wong, C.S.C., Zhang, W.L., 2005. Heavy metal and Pb isotopic compositions of aquatic organisms in the Pearl River Estuary, South China. Environ. Pollut. 138, 494–504.
Ip, C.C.M., Li, X.D., Zhang, G., Wai, O.W.H., Li, Y.-S., 2007. Trace metal distribution in sediments of the Pearl River Estuary and the surrounding coastal area, South China. Environ. Pollut. 147, 311–323.
Kritee, K., Blum, J.D., Johnson, M.W., Bergquist, B.A., Barkay, T., 2007. Mercury stable isotope fractionation during reduction of Hg(II) to Hg(0) by mercury resistant microorganisms. Environ. Sci. Technol. 41, 1889–1895.
Kritee, K., Barkay, T., Blum, J.D., 2009. Mass dependent stable isotope fractionation of mercury during mer mediated microbial degradation of monomethylmercury. Geochim. Cosmochim. Acta 73, 1285–1296.
Laffont, L., Sonke, J.E., Maurice, L., Hintelmann, H., Pouilly, M., Bacarreza, Y.S., Perez, T., Behra, P., 2009. Anomalous mercury isotopic compositions of fish and human hair in the Bolivian Amazon. Environ. Sci. Technol. 43 (23), 8985–8990.
Lawson, N.M., Mason, R.P., 1998. Accumulation of mercury in estuarine food chains. Biogeochemistry 40, 235–247.
Li, P., Feng, X.B., Qiu, G.L., Shang, L.H., Li, Z.G., 2009. Mercury pollution in Asia: a review of the contaminated sites. J. Hazard. Mater. 168, 591–601.
Liang, L., Horvart, M., Feng, X.B., Shang, L.H., Li, H., Pang, P., 2004. Re-evaluation of distillation and comparison with HNO3 leaching/solvent extraction for isolation of methylmercury compounds from sediment/soil samples. Appl. Organomet. Chem. 18 (6), 264–270.
Lindqvist, O., Johansson, K., Bringmark, L., Timm, B., Aastrup, M., et al., 1991. Mercury in the Swedish environment — recent research on causes, consequences and corrective method. Water Air Soil Pollut. 55, Xi-261.
Luis, R., Jesusa, R., Isaac, A., Laura, R.-C., 2007. Capability of selected crop plants for shoot mercury accumulation from polluted soils: phytoremediation perspectives. Int. J. Phytoremediation 9, 1–13.
Macleod, M., Mckone, T.E., Mackay, D., 2005. Mass balance for mercury in the San Francisco Bay Area. Envrion. Sci. Technol. 39, 6721–6729.
Mason, R.P., Lawson, N.M., Lawrence, A.L., Leaner, J.J., Lee, J.G., Sheu, G.R., 1999. Mercury in the Chesapeake Bay. Mar. Chem. 65, 77–96.
Mason, R.P., Kim, E.-H., Cornwell, J., Heyes, D., 2006. An examination of the factors influencing the flux of mercury, methylmercury and other constituents from estuarine sediment. Mar. Chem. 102, 96–110.
Merritt, K.A., Amirbahman, A., 2007. Mercury dynamics in sulfide-rich sediments: geochemical influence on contaminant mobilization within the Penobscot River estuary, Maine, USA. Geochim. Cosmochim. Acta 71, 929–941.
NDRC, National Development and Reform Commission, 2008. The Pearl River Delta reform development project summary (2008–2020).
Niessen, S., Foucher, D., Clarisse, O., Fischer, J.C., Milcac, N., Kwolcal, Z., Fajon, V., Horvat, M., 2003. Influence of sulphur cycle on mercury methylation in estuarine sediment (Science estuary, France). J. Phys. IV 107, 953–956.
Perrot, V., Epov, V.N., Pastukhov, M.V., Grebenshchikova, V.I., Zouiten, C., Sonke, J.E., Husted, S.r., Donard, O.F.X., Amouroux, D., 2010. Tracing sources and bioaccumulation of mercury in fish of Lake Baikal, Angara River using Hg isotopic composition. Envrion. Sci. Technol. 44 (21), 1212–1216.
Pickhardt, P.C., Fisher, N.S., 2007. Accumulation of inorganic and methylmercury by freshwater phytoplankton in two contrasting water bodies. Environ. Sci. Technol. 41, 125–131.
Schauble, E.A., 2007. Role of nuclear volume in driving equilibrium stable isotope fractionation of mercury, thallium, and other very heavy elements. Geochim. Cosmochim. Acta 71, 2170–2189.
Sherman, L.S., Blum, J.D., Nordstrom, D.K., McCleskey, R.B., Barkay, T., Vetriani, C., 2009. Mercury isotopic composition of hydrothermal systems in the Yellowstone Plateau volcanic field and Guaymas Basin sea-floor rift. Earth Planet. Sci. Lett. 279, 86–96.
Shi, J.B., Liang, L., Jiang, G., Jin, X., 2005. The speciation and bioavailability of mercury in sediments of Haihe River, China. Environ. Int. 31, 357–365.
Shi, Q., Rueckert, P., Leipe, T., Zhou, D., Harff, J., 2007. Distribution and contamination assessment of Hg in the sediments of the Pearl River Estuary. Mar. Environ. Sci. 26, 553–556 (In Chinese, abstract in English).
Shi, Q., Thomas, L., Peter, R., Zhou, D., Jan, H., 2010a. Geochemical sources, deposition and enrichment of heavy metals in short sediment cores from the Pearl River Estuary, Southern China. J. Mar. Syst. doi:10.1016/j.jmarsys.2010.02.003.
Shi, J.-B., Ip, C.C.M., Zhang, G., Jiang, G.B., Li, X.D., 2010b. Mercury profiles in sediments of the Pearl River Estuary and the surrounding coastal area of South China. Environ. Pollut. 158, 1974–1979.
Smith, C.N., Kesler, S.E., Klaue, B., Blum, J.D., 2005. Mercury isotope fractionation in fossil hydrothermal systems. Geology 33, 825–828.
Smith, C.N., Kesler, S.E., Blum, J.D., Rytuba, J.J., 2008. Isotope geochemistry of mercury in source rocks, mineral deposits and spring deposits of the California Coast Ranges, USA. Earth Planet. Sci. Lett. 269, 398–406.
Sonke, J.E., Schäfer, J., Chmeleff, J., Audry, S., Blanc, G., Dupré, B., 2010. Sedimentary mercury stable isotope records of atmospheric and riverine pollution from two major European heavy metal refineries. Chem. Geol. 279, 90–100.
Stetson, S.J., Gray, J.E., Wanty, R.B., Macalady, D.L., 2009. Isotopic Variability of mercury in ore, mine-waste calcine, and leachates of mine-waste calcine from areas mined for mercury. Environ. Sci. Technol. 43, 7331–7336.
Streets, D., Hao, J., Wu, Y., Jiang, J., Chan, M., Tian, H., Feng, X., 2005. Antropogenic mercury emissions in China. Atmos. Environ. 39, 7789–7806.
Sunderland, E.M., Mason, R.P., 2007. Human impacts on open ocean mercury concentrations. Glob. Biogeochem. Cycles 21, GB4022.
Tomiyasu, T., Nagano, A., Yonehara, N., Sakamoto, H., Rifardi, Oki, K., 2000. Mercury contamination in the Yatsushiro Sea, south-western Japan: spatial variations of mercury in sediment. Sci. Total Environ. 257, 121–132.
Ullrich, S.M., Tanton, T.W., Abdrashitova, S.A., 2001. Mercury in the aquatic environment: a review of factors affecting methylation. Crit. Rev. Envrion. Sci. Technol. 31, 241–293.
Ullrich, S.M., Ilyushchenko, M.A., Uskov, G.A., Tanton, T.W., 2007. Mercury distribution and transport in a contaminated river system in Kazakhstan and associated impacts on aquatic biota. Appl. Geochem. 22, 2706–2734.
Yang, L., Sturgeon, R., 2009. Isotopic fractionation of mercury induced by reduction and ethylation. Anal. Bioanal. Chem. 393, 377–385.
Yin, R.S., Feng, X.B., Foucher, D., Shi, W.F., Zhao, Z.Q., Wang, J., 2010. High precision determination of mercury isotope ratios using online mercury vapor generation system coupled with multicollector inductively coupled plasma-mass spectrometer. Chin. J. Anal. Chem. 38 (7), 929–934.
Zambardi, T., Sonke, J.E., Toutain, J.P., Sortino, F., Shinohara, H., 2009. Mercury emissions and stable isotopic compositions at Vulcano Island (Italy). Earth Planet. Sci. Lett. 277, 236–243.
Zelewski, L.M., Benoit, G., Armstrong, D.E., 2001. Mercury dynamics in Tivoli South Bay, a freshwater tidal mudflat wetland in the Hudson River. Biogeochemistry 52, 93–112.
Zhang, L., Wong, M.H., 2007. Environmental mercury contamination in China: sources and impacts. Environ. Int. 33, 108–121.
Zheng, W., Foucher, D., Hintelmann, H., 2007. Mercury isotope fractionation during volatilization of Hg(0) from solution into the gas phase. J. Anal. At. Spectrom. 22, 1097–1104.
Zhou, H.Y., Wong, M.H., 2000. Mercury accumulation in freshwater fish with emphasis on the dietary influence. Wat. Res. 34 (17), 4234–4242.